

# Does ocean-atmosphere coupling influence the properties of Tropical Instability Waves?

Luciano P Pezzi<sup>1</sup>

<sup>1</sup>*Centro de Previsão do Tempo e Estudos Climáticos - CPTEC  
Instituto Nacional de Pesquisas Espaciais - INPE  
Rod. Presidente Dutra Km 40 – 12630-00 - Cachoeira Paulista, SP*

luciano@cptec.inpe.br

**Abstract.** *In this study it is investigated how the modulation of surface wind-stress by tropical instability waves (TIWs) feeds back onto TIWs and plays a role in their fundamental properties. An ocean general circulation model is used, that reproduces qualitatively well the properties of TIWs when forced by climatological winds. The ocean model is coupled to the atmosphere through a simple parameterization of the wind stress response to SST. The properties of the TIWs in the coupled simulations are compared with those without active coupling. Active coupling results in a negative feedback on TIWs, reducing their variability, both at the surface and sub-surface. This reduced activity modulates the meridional heat and momentum transport, resulting in modest changes to the mean state, with a cooler cold tongue and stronger equatorial currents.*

**Resumo.** *Resultados de um modelo acoplado, usando um esquema simplificado da camada limite planetária (CLP) sob diferentes intensidades de acoplamento, sugerem que este sistema é capaz de simular as impressões atmosféricas das Ondas de Instabilidade Tropical (OIT) usando o coeficiente de acoplamento padrão. O acoplamento ativo produz um feedback negativo nas OIT. A atividade das OIT tendem a serem reduzidas tanto na superfície quanto na sub-superfície oceânica. Os experimentos usando acoplamento ativo simulam uma região do Pacífico equatorial mais fria (anomalias de até  $-0.3^{\circ}\text{C}$ ) comparadas com o experimento de controle (CTL). Entretanto, o mecanismo que explica completamente os efeitos das OIT na CLP precisa ser mais estudado.*

## 1. Introduction

TIWs and associated vortices are an oceanic phenomenon originated from the shear instabilities of the equatorial ocean current system. While great attention has been given to the oceanic signal, several studies have shown that there are signals of TIW activity in the lower atmosphere, within the atmospheric planetary boundary layer (ABL). These include surface wind modulation, water vapor and nebulosity. Studies investigating the SST influence on surface winds over the eastern equatorial Pacific were made in the late 80's by Lindzen and Nigam (1987), Hayes et al. (1989) and Wallace et al. (1989). These studies have proposed mechanisms for the interaction between the TIW oceanic signals and atmospheric signals.

One hypothesis (Lindzen and Nigam, 1987) attributes surface wind modulations to the variations in the Sea Level Pressure (SLP) field, linked to the TIW SST signals. Lower (high) pressures are found over warmer (cooler) water and as a consequence the strongest wind should be found at the highest pressure or SST gradients. The second hypothesis stated by Wallace et al. (1989) and Hayes et al. (1989) is that TIW SST anomalies induce ABL stability changes which in turn affect the wind variability. In this hypothesis air buoyancy is increased over the warmer waters, reducing the wind shear in the boundary layer thus producing stronger winds at the surface. Strongest winds should be found over warmest waters. Wallace et al. (1989) showed the antisymmetry in the climate over the eastern Pacific with the cold tongue SST being centered at  $1^{\circ}\text{S}$  and a strong frontal region centered at  $2^{\circ}\text{N}$ . The boundary layer air originating over the cold tongue (southern hemisphere) crosses meridionally the equatorial region and joins the Intertropical Convergence Zone (ITCZ) around  $8^{\circ}\text{N}$ . All these systems tend to be stronger during the cold season, which extends from July to November, when the meridional asymmetries are strongest. The oceanic frontal zone becomes hydrodynamically unstable, giving rise to westward propagating waves with periods of a few weeks. The atmospheric boundary layer undergoes a transition from a stable condition to an unstable condition as the air flows from the cold region to the warm (NECC) region across the SST front.

Xie et al. (1998) have studied the impact of these waves on the atmospheric boundary layer, analyzing the output from an AGCM averaged over the last 400 days of integration, satellite derived SST and wind data on a weekly time scale. The AGCM was able to reproduce roughly the wind field and divergence when compared with the satellite observations. Their results showed atmospheric waves with shallow vertical structure trapped in the ABL and that the ocean-atmosphere coupling happens on time-scales shorter than one month. TIW affects the horizontal wind direction and intensity in the ABL while ENSO modes affect the large scale atmospheric circulation, modifying the deep convection.

Recently, some key points of the TIWs have been studied using state of art data collected by satellite. The question concerning the ocean atmosphere interactions and influence of the TIWs on the surface wind has been revisited by Liu et al. (2000) and Chelton et al. (2001) and the TIWs themselves by Chelton et al. (2000). Many of these studies have used data from the microwave imager sensor TMI onboard the joint US/Japan Tropical Rainfall Measuring Mission (TRMM) satellite. This satellite sensor has been observing the Earth, mainly in the tropical region, in the spectral band of 10.7-85.0 GHz. The SST data have a daily temporal resolution and high spatial (approximately 46 Km) resolution. The atmosphere is nearly transparent to microwave radiation allowing SST data to be collected in all weather situations, except in rainy conditions. In other words, the atmosphere is seen free of clouds in nonraining situations allowing the acquisition of a nearly uninterrupted time series.

Using satellite-derived data Liu et al. (2000) clearly showed the manifestation of TIWs over the northern front of the Pacific cold tongue and using a zonal band pass filter they were able to isolate the TIW signal in SST, wind components and wind speed to analyze the phase propagation differences. They found in a region between  $1.5^{\circ}\text{N}$  to  $3.5^{\circ}\text{N}$  and  $105^{\circ}\text{W}$  to  $145^{\circ}\text{W}$  SST that was in phase with the wind speed whilst the meridional component of the wind was out of phase ( $-155^{\circ}$ ). The wind response to the SST

gradients is shown in Liu et al. (2000). As the wind moves over these SST anomalies it is accelerated and decelerated producing centers of convergence and divergence at maxima SST gradient regions. The convergence maxima (minima) also coincide with the water vapor maxima (minima), where convergence (divergence) feeds (withdraws) the water vapor up in the atmosphere increasing (decreasing) the instability in the air column. The water vapor increase in this region might be a consequence of the warm waters and air advection. Based on their findings Liu et al. (2000) suggest that the modification of the surface winds is due to the ABL stability changes, agreeing with Wallace et al. (1989).

These results have been corroborated by Hashizume et al. (2002) using a sequence of atmospheric radiosondings of air temperature, humidity and wind obtained during a cruise sailing through developed TIWs in the Pacific Ocean. From their Figure 9, can be seen that the atmospheric response to TIWs extends through the whole ABL and modulates its vertical extension. Over warm waters the atmospheric boundary layer is unstable increasing the vertical mixing and the ABL height. The turbulence within the vertical column increases also and more momentum is transferred downwards decreasing the vertical shear and accelerating the surface wind over warmest waters in agreements with the previous studies.

Recently, Small et al. (2003) have re-opened the discussion about which mechanism is prevailing in the wind surface modulation. Using a high resolution regional climate model with improved physics and forced by TMI SST have examined the atmospheric impacts to Pacific TIWs. Their results suggest that horizontal advection changes the SLP phase relation with SST, the high and low pressure centers are located downwind of the cold and warm SST anomalies centers. Also their momentum budget analysis suggests that pressure gradient term is dominating the balance, besides of the vertical mixing and horizontal advection.

The differences and similarities of the TIWs in the Pacific and Atlantic oceans have been explored by Hashizume et al. (2001) also using the TMI sensor during the second half of 1999, when a well established La Niña was present in the Pacific. The cold tongue in the Atlantic has a faster development and decay than that in the Pacific. Possibly associated to climatic and climatological differences, the wavelength of the Atlantic TIW is smaller ( $9^\circ$  of longitude) when compared with the Pacific ( $12^\circ$ ). It was also observed that in both oceans TIW activity has some indirect impact on the southern edge of the ITCZ.

Thus, while many studies in the past have shown that TIWs originate from oceanic instabilities the discussion above show that there is also an imprint of TIWs in the atmosphere via mainly ABL stability modulations. In this study, we explore the ocean-ABL coupled interactions and the main points addressed here are; Does ocean-atmosphere coupling influence the properties of Tropical Instability Waves? Are those ocean-atmosphere couplings just impacting the PBL or are they closed loop with the PBL impacting on the TIW oceanic characteristics? We chose to study the TIW ocean-atmosphere interactions using an OGCM coupled with a simplified statistical ABL scheme.

The remainder of this study is organized as follow. In Section 2 the ocean model configuration, ABL scheme formulism, coupling coefficients calculation and system setup are presented. In Section 3 the model spin-up and sensitivity experiments are described.

In Section 4 the equatorial current system, TIW simulations and variability are analyzed. A brief summary and conclusions are presented in the last section (Section 5).

## 2. Model configurations

### 2.1. Ocean Model

In this study we use the LODYC Ocean General Circulation Model (OGCM) (Madec et al., 1998) in a tropical Pacific configuration. However, it has a slightly different grid configuration and a brief description of the main characteristics follows.

The domain used for this study is similar to the one used in Pezzi and Richards (2003). It covers the tropical Pacific from 30°S to 30°N and from 130°E to 70°W, with realistic representation of coastlines. The meridional resolution is 0.5° in the equatorial belt from 5°S to 5°N increasing grid space up to 2° at the southern and northern boundaries. The resolution in zonal direction is 1°, equally grid spaced along the domain. The model has 31 levels in the vertical, with the highest resolution of approximately 10 meters in the top 150 meters. Below this depth the resolution decreases down to 500 meters near the ocean bottom at 5000 meters. The lateral mixing for tracers and momentum is applied along isopycnal surfaces following the scheme described in Lengaigne et al. (2003). The mixing coefficient used is  $2 \times 10^3 \text{ m}^2\text{s}^{-1}$ . The results produced by the isopycnal mixing parameterization have suggested a better representation of the eddy effects in the equatorial region and of the tropical circulation, as suggested by Lengaigne et al. (2003).

### 2.2. The coupling scheme

In order to investigate whether the ABL-TIW induced patterns do influence the TIWs themselves we assess the differences between experiments forced by specified wind stress and experiments where a ocean-ABL coupling scheme at the TIW scale has been introduced. The experiments are run with the wind stress specified as follows:

$$\tau = \tau_0 + \begin{pmatrix} \alpha SST' \\ \beta SST' \end{pmatrix} \quad (1)$$

where  $\tau_0$  is the October climatological wind stress used for the control experiment and  $SST'$  is the difference between the model SST at a particular instant with the long term averaged  $\overline{SST}$  from the control experiment. The  $\alpha$  and  $\beta$  values in Equation 1 used for these experiments are given in Table 2. The zonal and meridional coupling coefficients used in STD experiment are computed from a statistical regression between the 10-50 days filtered Quikscat wind stress and TRMM SST at 140°W, 2°N (the region where the highest correlation of 0.5 between these two data set was found) covering the period 1999-2001. This is an approach similar to that used in Hashizume et al. (2001) and Polito et al. (2001) but here it is applied to relate wind stress (rather than wind) to SST. While we are aware that this is a very crude approach, the results obtained with our simplified scheme produces wind stress anomalies consistent with the magnitude and spatial patterns found in observations. In one way of the ocean-atmosphere coupling, the ABL scheme can be forced by SST produced by the oceanic model and those are included in the wind

calculations. On the other way the ABL returns back the wind stress to force the ocean model closing the ocean-atmosphere coupling loop. A simple formulism to calculate the surface wind stresses based on a given background wind plus the information coming from the ocean through SST anomalies is used.

Experiments	$\alpha$	$\beta$
STD	-0.02	0.008
MID	-0.03	0.012
HIG	-0.05	0.020

**Tabela 1: Linear regression coefficients calculated from the TMI SST and Quicks-cat scatterometer. Time series data are coincident in time, covering the period from June 1999 to December 2001, and space.  $\alpha$  and  $\beta$  represent the zonal and meridional directions, respectively.**

The preliminary results have shown considerable differences on the simulated mean state when different experiments are compared. The question that arose is; are the differences seen in the mean state caused by the TIWs feedback themselves or caused by the coupling effects in the regions outside of the TIW activity region?

In order to minimize the ABL coupling impacts on the oceanic mean state, the active coupling region is restricted to an equatorial area where the TIWs are generated. The ITCZ is located northward of this area and the coupling mechanisms may differ. Thus,  $\alpha$  and  $\beta$  are defined as function of the latitude and longitude limits respectively. The coefficient values are multiplied by one within a region chosen for active coupling region, extending from 9°S to 9°N and from 160°E to 90 °W, and zero elsewhere. In order to avoid an abrupt change in the active coupling a 3° wide transition zone decaying to zero in all four directions (north, south, east and west borders) is applied.

### 3. Experiments performed

#### 3.1. Spin-up and control experiments

The ocean model is first spun-up with October climatological wind stress forcing ERS+TAO (Menkes et al., 1998), starting from rest and Levitus and Boyer (1994) temperature and salinity. The net heat flux is parameterized as a relaxation towards October climatological SST observations (Levitus and Boyer, 1994) using a relaxation coefficient of  $-40 \text{ W m}^{-2}\text{K}^{-1}$ . There is no relaxation to climatological salinity. The results are analyzed after the 60<sup>th</sup> year of integration when the solution has reached a statistically quasi-steady state.

In order to be coherent with the sensitivity experiments comparison, an additional two years experiment is performed restarting from the spin-up and with  $\alpha$  and  $\beta$  set to zero. The only variability in this experiment is linked to tropical instability waves and will be further described in Section 4.

#### 3.2. Coupled experiments

Three two-years experiments are performed with non-zero values of  $\alpha$  and  $\beta$ , i.e. allowing a coupling between the ocean and the atmospheric boundary layer. The  $\alpha$  and  $\beta$

values used for these experiments are given in Table 2. The zonal and meridional coupling coefficients used in the STD experiment are the values computed from the statistical regression as defined in the Section 2.2. In experiment MID, the coefficients are multiplied by a factor of 1.5 and in the HIG, they are multiplied by a factor of 2. The effects of ABL coupling for each case are compared with the control run experiment (CTL). The 60<sup>th</sup> spin-up year which used constant October forcing is used as initial conditions. The coupled experiments differ only in the coupling strength applied, all the other parameters and configurations are kept identical.

## 4. Results

In this section, we first show that the TIWs in our experiments have properties consistent with observations and that the simple coupling approach used reproduces qualitatively the wind response to TIWs. After, we assess how the coupling modifies the TIW properties. Finally, we investigate how the change of TIW properties feedback onto the mean state of the model.

### 4.1. The simulated TIWs and wind response

Figure 1 shows a snapshot of the SST, surface currents and wind stress signals in the region of TIW activity, for the STD experiment. The filtering used is based on a Finite Impulse Response (FIR) 2-D digital filter, e.g. Polito et al. (2000), selecting zonal scales ranging from 5° to 25° and periods from 10 to 80 days.

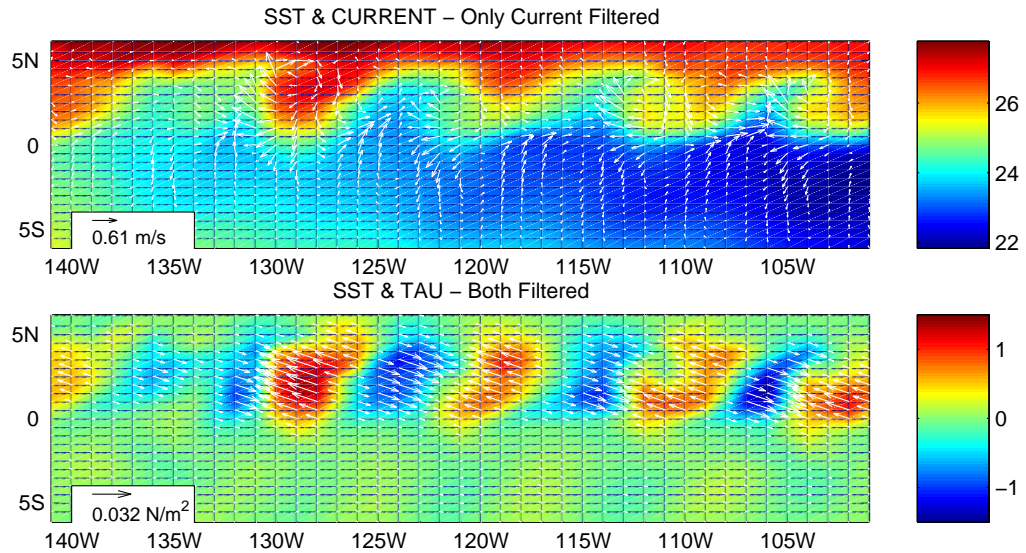


**Figure 1: SST with filtered currents superimposed (upper panel). SST and wind stress superimposed, both filtered fields (lower panel). STD experiment**

The model simulates the gross features of the cold tongue, as shown in Figure 1 (upper panel), and also exhibits a well defined cusp-shaped wave pattern similar to the TIW patterns described in the literature (Chelton et al., 2000). However the model does underestimate the TIW activity south of the equator. The TIWs propagate westward in

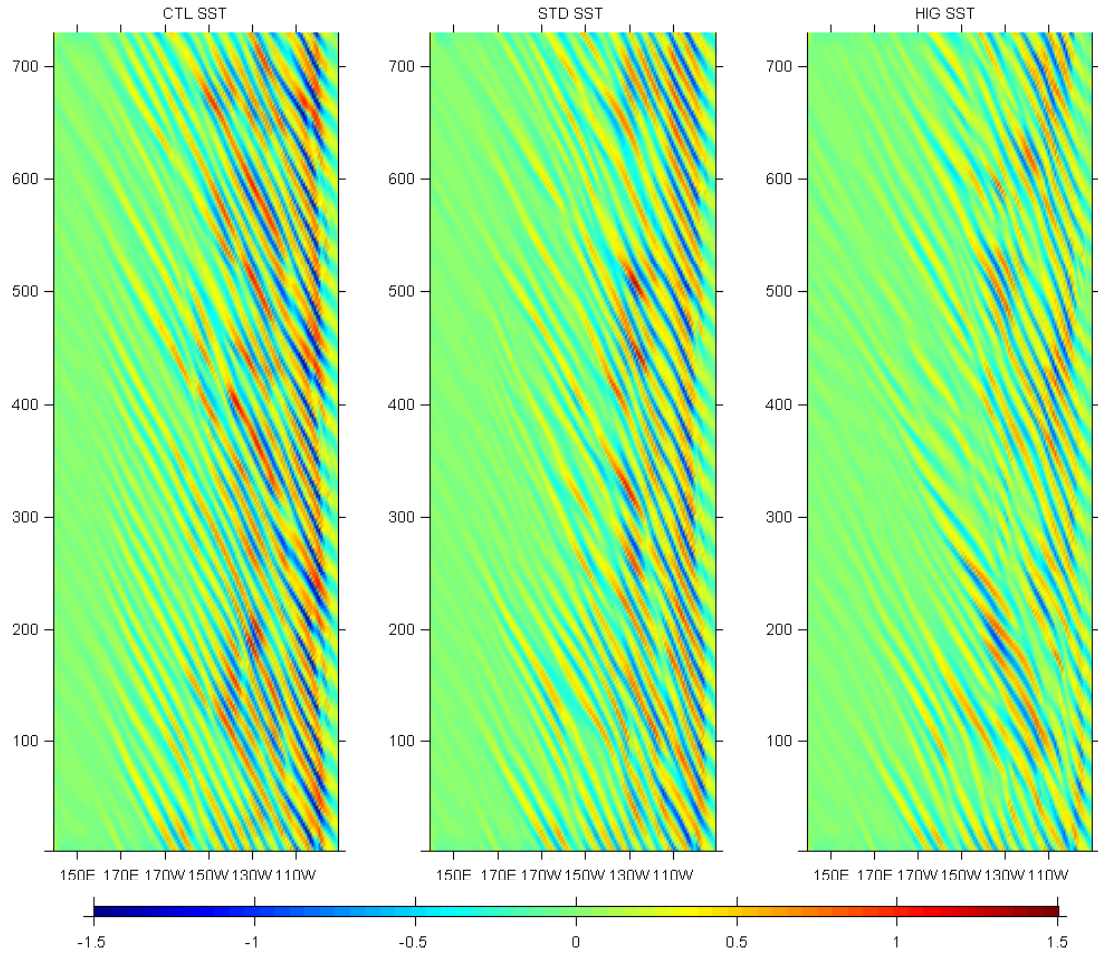
all experiments (e.g. Figure 2). The phase propagation speed of the waves is around  $30 \text{ cm s}^{-1}$ , in the lower values of the observed speed ranges (Chelton et al., 2000, Kennan and Flament, 2000). The period of the TIWs is around 30 days also in good agreement with estimates from observations (Qiao and Weisberg, 1995). Overall, the properties of the TIW activity in the control experiment, CTL, are consistent with Vialard et al. (2003) and Pezzi and Richards (2003).

Figure 1 (lower panel) shows anomalous patterns of wind stress superimposed on anomalous patterns of SST in experiment STD. The wind is increased over warm water and decreased over cold water. This results in convergence and divergence centers over the SST gradients, consistent with what is found in observations (compare Figure 4 in Liu et al. (2000) with Figure 1). This is also discussed by Chelton et al. (2001) who show the wind stress curl perturbations associated with TIWs. The typical amplitude of the wind stress anomalies in STD is  $0.03 \text{ N m}^{-2}$ , corresponding to a 25% modulation of the  $0.12 \text{ N m}^{-2}$  October climatological wind stress in the  $100^{\circ}\text{W}$ - $140^{\circ}\text{W}$ ,  $0^{\circ}$ - $5^{\circ}\text{N}$  region. The amplitude of the anomalies is consistent with the observations described by Chelton et al. (2001) (see Figure 14b), which shows TIW-induced stress perturbations of the magnitude obtained by the coupling parameterization used in this study. The simple approach we chose for introducing the coupling therefore produces a response which is in reasonable agreement with the observed wind stress response to the SST signal of TIWs, both in pattern and amplitude. In the next section, we will start evaluating how this coupled response influences the TIWs.

#### 4.2. Impact of coupling on TIW variability

The CTL experiment exhibits larger SST variability than the two coupled experiments, especially in the eastern portion of the domain, as shown in Figure 2. Changes in variabilities are illustrated in Figure 3 which allows a more quantitative estimate of the level of variability in temperature and currents over the active TIWs region. Only the CTL and HIG experiments are shown. Active coupling results in a clear diminution of the temperature variability, especially above the thermocline and near the surface (Figure 3). The meridional velocity variability is also clearly reduced, both close to the surface and around 100 m. At the surface, this reduction is most obvious close to the equator. The zonal current variability, on the other hand, is increased. This increase is most obvious around  $4^{\circ}\text{N}$ , *i.e.*, on the northern side of the eddies depicted in Figure 1. A possible explanation for the changes in the surface current activity is that they are linked to changes in the Ekman flux driven by the atmospheric response to TIWs. Indeed the direction of the Ekman flux resulting from the wind stress anomalies in Figure 1 tends to strengthen the zonal current and to weaken the meridional current. This simple argument provides an explanation for the qualitative changes in the variance of the currents, but not the detail (it does not explain for instance the stronger increase of the zonal current to the north, nor changes in meridional current below the Ekman layer). The change in the temperature activity is consistent with the TIW heat budget analysis of Kennan and Flament (2000) where the meridional heat flux is the main contributor to generating temperature variability associated with TIWs. The reduction of the meridional current activity in coupled experiments is consistent with the reduced temperature variability. Although there are significant changes in the amplitude of the TIWs and the associated fluxes of heat and momentum, the wavelength and phase speed of the TIWs are little changed when the





**Figura 2: Filtered time-longitude SST displaying TIWs for the CTL, STD, and HIG experiments averaged over the latitudinal band from 1°N to 3°N. Units are °C.**

coupling is introduced and do not show a clear tendency when the strength of the coupling is increased.

#### 4.3. Rectification of the mean state

Table 2 shows a number of gross measures of mean state and how they vary with the strength of the coupling. Increasing the strength of the coupling leads to a decrease in

Variable	CTL	STD	MID	HIG
EUC	61	68	70	77
SEC	-52	-53	-52	-59
$SST_v$	23.3	23.1	23.0	22.9

**Tabela 2: Maximum values of current speed ( $\text{cm s}^{-1}$ ) for each experiment.  $SST_v$  represents the averaged temperature in the box extending from 120°W to 100°W, 0 to 6°N and from surface down to 140 m.**

the SST of the cold tongue. There are two competing effects of the coupling on the cold



tongue SST. The first is a reduction in the equatorward meridional flux of heat by the TIWs. The temperature flux  $\langle T'v' \rangle$  is decreased by 38%, between CTL and HIG (not shown) consistent with the reduction in the  $\langle T \rangle$  and  $\langle v \rangle$  variability, Figure 3. This changes implies cooling south of  $3^\circ\text{N}$  and a warming north of  $3^\circ\text{N}$  relative to the control run which is consistent with the cooling of the cold tongue as the coupling is increased. The second effect is a reduction in the upwelling of cold water brought about by the reduction in surface stress over the colder SST. This reduction in upwelling is 30% between CTL and HIG, and would imply a warming of the cold tongue. In fact the changes to the cold tongue temperature are dominated by changes to the TIWs. Regarding the mean

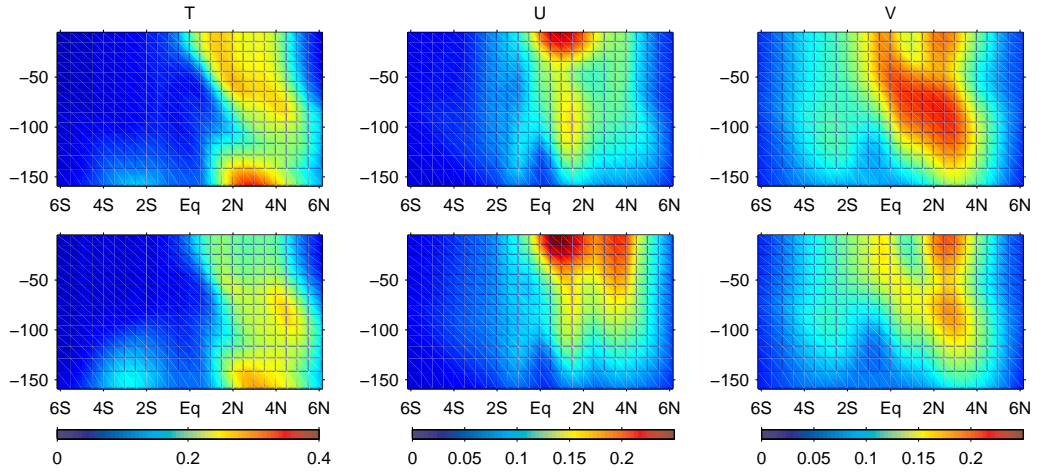


**Figure 3: The standard deviation zonally averaged over the region ranging from  $150^\circ\text{W}$  to  $90^\circ\text{W}$ , represented by  $\langle \rangle$ , CTL (upper row) and HIG (lower row) experiments.  $\langle T \rangle$  on the left ( $^\circ\text{C}$ ),  $\langle u \rangle$  on the central column and  $\langle v \rangle$  on the right ( $\text{m s}^{-1}$ ).**

currents, the SEC does not display any significant change in STD and MID, though it does increase in HIG. The coupling impact on the SEC is thus neutral or a slight increase of the current intensity. On the other hand, the EUC is significantly increased in all the experiments with active coupling (by more than 25% between CTL and HIG). This increase in the mean EUC is consistent with the decrease in the divergence of  $\langle u'v' \rangle$  close to the equator around 100 meters depth as the coupling strength is increased (Figure 3), i.e. the decreased TIW activity retards the mean flow less. Similarly, the decrease in the convergence close to the surface (around  $2^\circ\text{N}$ ) is consistent with the increase in the westward SEC seen in experiment HIG.

Finally we ask the question: are the changes to the TIW activity a direct result of the coupling of the TIWs and the atmosphere, which in turn affects the mean state, or are they associated with changes in the forcing on the broader scale (a form of ‘climate drift’ of the model), where changes in the mean state affect the TIW activity? The results presented above are consistent with the first alternative, but to fully answer the question we have performed additional experiments as follows. The wind forcing of each coupled experiment is low-pass filtered and used to force a new control experiment, with no active coupling, but retaining the low-frequency changes due to climate drift. The results show no significant change in the amplitude of TIW variability (compared to CTL). We

therefore conclude that the bulk of the change in TIW variability is a result of the active coupling and not to changes in the mean state.

## 5. Discussion

A simple wind stress parameterization, sensitive to SST patterns, has been used to investigate if the observed modulation of surface fluxes by TIWs has any impact on the properties of the waves themselves. Despite the simplicity of the parameterization scheme we find a broad agreement between the model and observations in terms of the properties of the TIWs and their imprint in the pattern of wind stress. Active coupling between the ocean and atmospheric boundary is found to produce a significant reduction in the activity of the TIWs in both amplitude and longitudinal extent. The coupling increases the zonal current and decreases the meridional current activity. This response is largely consistent with the changes in Ekman transport associated with the wind stress modulation. The reduced meridional current variability results in reduced meridional undulations of the equatorial SST front, and thus reduced temperature activity.

The reduced TIW activity changes the meridional heat and momentum transport, leading to changes in the mean state (a cooler cold tongue SST and stronger EUC as the coupling is increased). The effects are moderate (an increase of around 10% in the strength of the EUC for moderate values of the coupling), but significant. The trend in the cold tongue SST with strength of coupling highlights the complexity of the equatorial system and how difficult it is to *a priori* estimate how changes to the system will affect its behavior, without careful numerical experimentation. The coupling between the atmospheric boundary layer and surface ocean affects the system in a number of ways. Here we find the broadscale effects of reduced wind stress, and associated upwelling, overwhelmed by the effects of the reduced TIW activity.

There are a number of caveats to this study. Among them is that we chose to investigate only the impact of the wind stress modulation on the TIWs. The heat flux feedback is parameterised in all the experiments in a similar way by a relaxation to climatological SST. This is a rather crude parameterisation of the flux modulation by the TIWs variability. For example, phase differences between the TIW SST anomalies and atmospheric flux response could be expected because of the modulation of surface winds and humidity by the TIWs, see Thum et al. (2002). Similarly, the parameterisation of the wind stress response in this study is very crude. Despite its relative success in reproducing the observed wind stress pattern, it probably oversimplifies the variety of atmospheric responses that can stem from the various ABL processes. Experiments with a more sophisticated coupled model should be undertaken, and will be done in a future study. However we contend that our results do demonstrate the importance of the coupling between the atmospheric boundary and upper ocean and the need to consider such effects in studies of the equatorial ocean.

## 6. acknowledgments

I would like to thank Prof. Kelvin Richards for his scientific advice throughout this project. Dr. Jerome Vialard, Dr. Christophe Menkes and Dr. David Anderson for encourage me to study TIWs under an ocean-atmosphere coupled perspec-

tive. The OPA development team at LODYC for providing the model source code (<http://www.lodyc.jussieu.fr/opa/index.html>), Claire Lévy for assistance with the software. This work was supported by the Conselho Nacional de Pesquisas - CNPq Brazil Grant Nr 200748/98-0.

## Referências

- Chelton, D. B., Esbensen, S. K., Schlax, M. G., Thun, N., Freilich, M., Wentz, F. J., Gentmann, C. L., McPhaden, M. J., and Schopf, P. S. (2001). Observations of coupling between surface wind stress and sea surface temperature in the eastern tropical pacific. *Journal of Climate*, 14:1479–1498.
- Chelton, D. B., Wentz, F. J., Gentemann, C. L., Szoek, R. A., and Schlax, M. G. (2000). Satellite microwave sst observations of transequatorial tropical instability waves. *Geophysical Research Letters*, 27(9):1239–1242.
- Hashizume, H., Xie, S. P., Fujiwara, M., Shiotani, M., Watanabe, T., Tanimoto, Y., Liu, W. T., and Takeuchi, K. (2002). Direct observations of atmospheric boundary layer response to sst variations associated with tropical instability waves over the eastern equatorial pacific. *Journal of Climate*, 15:3379–3393.
- Hashizume, H., Xie, S. P., Liu, W. T., and Takeuchi, K. (2001). Local and remote atmospheric response to tropical instability waves: A global view from the space. *Journal of Geophysical Research*, 106(D10):10173–10185.
- Hayes, S. P., McPhaden, M. J., and Wallace, J. M. (1989). The influence of sea surface temperature on surface wind in the eastern equatorial pacific: Weekly to monthly variability. *Journal of Climate*, 2:1500–1506.
- Kennan, S. C. and Flament, P. J. (2000). Observations of a tropical instability vortex. *Journal of Physical Oceanography*, 30:2277–2301.
- Lengaigne, M., Madec, G., Menkes, C., Jouzeau, A., and Alory, G. (2003). Impact of isopycnal mixing on the tropical ocean circulation. *submitted to Journal of Geophysical Research*.
- Levitus, S. and Boyer, T. (1994). World ocean atlas 1994. Tech. Report. (Salinity and Temperature) Vol 3-4, US Dep. of Commer., Washington, DC.
- Lindzen, R. S. and Nigam, S. (1987). On the role of sea surface temperature gradients in forcing low-level winds and convergence in the tropics. *Journal of the Atmospheric Sciences*, 44(17):2418–2436.
- Liu, W., Xie, X., Polito, P. S., Xie, S. P., and Hashizume, H. (2000). Atmospheric manifestation of tropical instability wave observed by quickscat and tropical rain measuring mission. *Geophysical Research Letters*, 27(16):2545–2548.
- Madec, G., Delecluse, P., Imbard, M., and Lvy, C. (1998). Opa8.1 ocean general circulation model - reference manual. *Notes du Pôle de Modélisation - Laboratoire d’Océanographie Dynamique et de Climatologie (LODYC)*, Note 11:93pp.
- Menkes, C., Boulanger, J.-P., Busalacchi, A. J., Vialard, J., Delecluse, P., McPhaden, M. J. M., Hackert, E., and Grima, N. (1998). Impact of tau vs ers wind stress onto simulations of the tropical pacific ocean during 1993-1998 period by the opa ogcm. *Euroclivar Workshop Rep.*, pages 46–48.
- Pezzi, L. P. and Richards, K. J. (2003). The effects of lateral mixing on the mean state and eddy activity of an equatorial ocean. *Journal of Geophysical Research*, 108(C12):doi:10.1029/2003JC001834.

- Polito, P., Ryan, J. P., Liu, W. T., and Chavez, F. P. (2001). Oceanic atmospheric anomalies of tropical instability waves. *Geophysical Research Letters*, 28(11):2233–2236.
- Polito, P., Sato, O. T., and Liu, W. T. (2000). Characterization and validation of the heat storage variability from topex/poseidon at four oceanographic sites. *Journal of Geophysical Research*, 105(C7):16911–16921.
- Qiao, L. and Weisberg, R. H. (1995). Tropical instability wave kinematics: Observations from the tropical instability wave experiment. *Journal of Geophysical Research*, 100(C5):8677–8693.
- Small, R. J., Xie, X.-P., and Wang, Y. (2003). Numerical simulation of atmospheric response to pacific tropical instability waves. *Journal of Climate*, Submitted.
- Thum, N., Esbensen, S. K., and Chelton, D. B. (2002). Air-sea heat exchange along the northern sea surface temperature front in the eastern tropical pacific . *Journal of Climate*, 15:3361–3378.
- Vialard, J., Menkes, C., Anderson, D. L. T., and Balmaseda, M. A. (2003). Sensitivity of pacific ocean tropical instability waves to initial conditions. *Journal of Physical Oceanography*, 33:105–121.
- Wallace, J. M., Mitchell, T. P., and Deser, C. J. (1989). The influence of sea-surface temperature on surface wind in the eastern equatorial pacific: Weekly to monthly variability. *Journal of Climate*, 2:1492–1499.
- Xie, S. P., Ishiwatari, M., Hashizume, H., and K., T. (1998). Coupled ocean-atmosphere waves on the equatorial front. *Geophysical Research Letters*, 25(20):3863–3866.